Gust Disturbance Alleviation with Incremental Nonlinear Dynamic Inversion

Conference Paper · October 2016

DOI: 10.1109/IROS.2016.7759827

3 authors:

Ewoud Jan Jacob Smeur
Technische Universität München
17 PUBLICATIONS **134** CITATIONS
SEE PROFILE

Guido de Croon
Delft University of Technology
156 PUBLICATIONS **1,387** CITATIONS
SEE PROFILE

Q. P. Chu
Delft University of Technology
249 PUBLICATIONS **2,663** CITATIONS
SEE PROFILE

2016 IEEE/RSJ International Conference on Intelligent Robots and Systems (IROS)
Daejeon Convention Center
October 9-14, 2016, Daejeon, Korea

Gust Disturbance Alleviation with Incremental Nonlinear Dynamic Inversion

Ewoud J.J. Smeur[1] and Guido C.H.E. de Croon[2] and Qiping Chu[3]

Abstract— **Micro Aerial Vehicles (MAVs) are limited in their operation outdoors near obstacles by their ability to withstand wind gusts. Currently widespread position control methods such as Proportional Integral Derivative control do not perform well under the influence of gusts. Incremental Nonlinear Dynamic Inversion (INDI) is a sensor-based control technique that can control nonlinear systems subject to disturbances. This method was developed for the attitude control of MAVs, but in this paper we generalize this method to the outer loop control of MAVs under gust loads. Significant improvements over a traditional Proportional Integral Derivative (PID) controller are demonstrated in an experiment where the drone flies in and out of a fan's wake. The control method does not rely on frequent position updates, so it is ready to be applied outside with standard GPS modules.**

I. INTRODUCTION

Micro Aerial Vehicles (MAV) have the potential to perform many useful tasks, such as search and rescue [1], package delivery, aerial imaging [2], etc. For applications where the MAV needs to operate close to obstacles or close to the ground, accurate position control is of paramount importance. However, currently widespread position control methods such as Proportional Integral Derivative control (PID) [3] do not perform well under the influence of gusts.

Imagine a search and rescue scenario where a drone needs to fly into a house through an open window to look for survivors of a disaster. If the conditions are windy outdoors, the drone will need to provide a certain force to counteract this wind. The moment the drone flies into the house, the drag from the wind disappears and the drone will start to accelerate. With traditional control methods, the drone is likely to hit something in a confined indoor space.

Outdoor UAV missions can encounter significant gusts due to atmospheric turbulence [4]. Shen et al. even observed these wind disturbances indoor [5], and they needed an augmentation of the controller that could cope with slowly varying wind disturbances. To cope with fast changing wind gusts, a solution could be to use onboard wind sensors to estimate the wind field [6]. However, this increases the system complexity and cost.

*This work was supported by the Delphi Consortium

[1]Ewoud J.J. Smeur is with Faculty of Aerospace Engineering, Delft University of Technology, 2629HS Delft, The Netherlands e.j.j.smeur@tudelft.nl

[2]Guido C.H.E. de Croon is with Faculty of Aerospace Engineering, Delft University of Technology, 2629HS Delft, The Netherlands G.C.H.E.deCroon@tudelft.nl

[3]Qiping Chu is with Faculty of Aerospace Engineering, Delft University of Technology, 2629HS Delft, The Netherlands q.p.chu@tudelft.nl

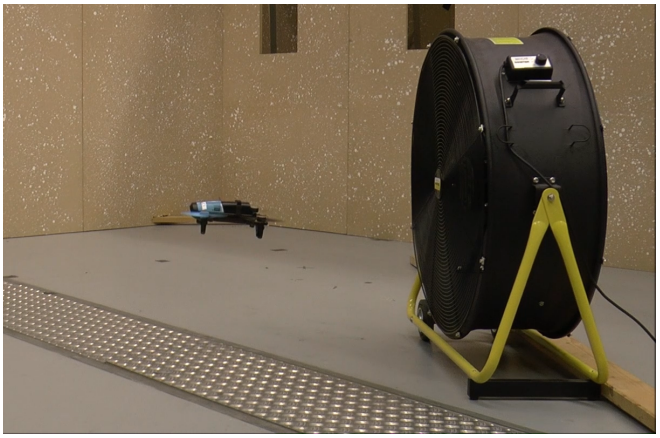

Fig. 1: The quadcopter in front of the fan during one of the experiments.

Alternatively, the wind velocity could be estimated onboard through modeling [7], [8]. The downside of this approach is that it is very dependent on the model. If the model does not represent reality well enough due to modeling errors or airframe changes, the gust alleviation performance will degrade. Gardner et al. focused on creating a framework to assess the ability of different physical platforms to withstand gusts [9], but they did not discuss how the controller can take advantage of this ability.

Hoffmann et al. showed that the vertical control of a quadrotor can be improved by using a gain on the vertical acceleration measurement [10]. Simplicio et al. improved on this idea by applying the method of Incremental Nonlinear Dynamic Inversion (INDI) to the vertical control of a helicopter using the main collective [11]. INDI is a sensor based control method that was developed for attitude control of aircraft [12]. Simplicio shows that the INDI altitude controller is able to track a reference in simulation, but no disturbance rejection properties are discussed. The approach of using the accelerometer seems promising, since disturbances are measured, as is pointed out by Wang et al. [13]. However, to fully take advantage of this fact, all axes should be taken into account.

In this paper we introduce a gust resistant controller through generalization of INDI to the outer loop control. This controller does not require any information on the aerodynamic drag of the quadrotor. It is implemented on a Parrot Bebop quadrotor running the Paparazzi open source autopilot software [14]. Experiments are performed that show only five cm position changes while entering and leaving

an industrial fan's wake. A benchmark PID controller gives position errors of half a meter for the same test.

II. Incremental Nonlinear Dynamic Inversion Applied to Linear Accelerations

Consider the quadrotor shown in Figure 2. The distance from the center of gravity to each of the rotors along the body X axis is given by l and along the Y axis by b. Two reference frames will be used throughout this paper, the body frame, with subscript B and the North East Down (NED) frame, with subscript N. The subscripts will only be used to avoid confusion, the position $\boldsymbol{\xi}$ and velocity $\boldsymbol{v}$ of the MAV will always be in the NED frame.

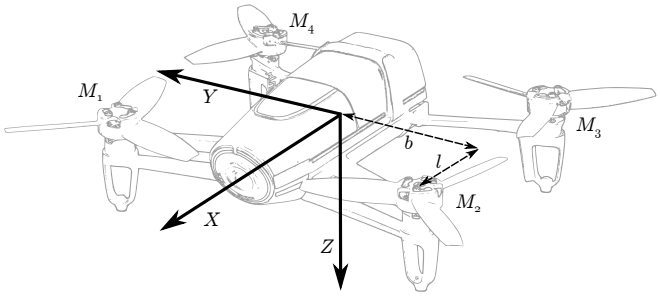

Fig. 2: The Bebop Quadcopter used in the experiments with body axis definitions.

We start with a description of the system, in this case the position dynamics. These follow from Newton's second law of motion:

$$m\ddot{\boldsymbol{\xi}} = m\boldsymbol{g} + \boldsymbol{F}(\boldsymbol{v}) + \boldsymbol{T}_N(\boldsymbol{\eta}, T) \tag{1}$$

Where $\boldsymbol{\xi} = [x, y, z]^T$ is the position and $\boldsymbol{F}$ is the aerodynamic force working on the airframe as a function of the velocity $\boldsymbol{v}$ of the MAV. $\boldsymbol{T}_N$ is the thrust vector in the NED frame as a function of the attitude $\boldsymbol{\eta} = [\phi, \theta, \psi]^T$ and the total thrust produced by the four rotors T. Finally, $\boldsymbol{g}$ is the gravity vector and m is the mass of the drone.

The thrust vector in the NED frame can be obtained by taking the thrust vector in the body frame, defined as $\boldsymbol{T}_B = [0, 0, T]^T$, and rotating it using the rotation matrix $\boldsymbol{M}_{NB}(\boldsymbol{\eta})$. Since the thrust vector in the body frame only has a Z component, only the last column of the rotation matrix is relevant. The thrust vector in the NED frame is therefore given by the following:

$$\boldsymbol{T}_N(\boldsymbol{\eta}, T) = \boldsymbol{M}_{NB}(\boldsymbol{\eta})\boldsymbol{T}_B = \begin{bmatrix} (\mathrm{s}\phi\mathrm{s}\psi + \mathrm{c}\phi\mathrm{c}\psi\mathrm{s}\theta)T \\ (\mathrm{c}\phi\mathrm{s}\psi\mathrm{s}\theta - \mathrm{c}\psi\mathrm{s}\phi)T \\ (\mathrm{c}\phi\mathrm{c}\theta)T \end{bmatrix} \tag{2}$$

where the sine and cosine functions are abbreviated by the letters s and c respectively.

Now we can apply a first order Taylor expansion to Eq. 1, resulting in Eq. 3.

$$\begin{aligned} m\ddot{\boldsymbol{\xi}} = \; & m\boldsymbol{g} + \boldsymbol{F}(\boldsymbol{v}_0) + \boldsymbol{T}_N(\boldsymbol{\eta}_0, T_0) \\ & + \tfrac{\partial}{\partial \boldsymbol{v}}\boldsymbol{F}(\boldsymbol{v})|_{\boldsymbol{v}=\boldsymbol{v}_0}(\boldsymbol{v} - \boldsymbol{v}_0) \\ & + \tfrac{\partial}{\partial \boldsymbol{\phi}}\boldsymbol{T}_N(\boldsymbol{\eta}, T)|_{\phi=\phi_0}(\phi - \phi_0) \\ & + \tfrac{\partial}{\partial \boldsymbol{\theta}}\boldsymbol{T}_N(\boldsymbol{\eta}, T)|_{\theta=\theta_0}(\theta - \theta_0) \\ & + \tfrac{\partial}{\partial T}\boldsymbol{T}_N(\boldsymbol{\eta}, T)|_{T=T_0}(T - T_0) \end{aligned} \tag{3}$$

The first three terms can be simplified to the acceleration due to the current state and input: $m\boldsymbol{g} + \boldsymbol{F}(\boldsymbol{v}_0) + \boldsymbol{T}_N(\boldsymbol{\eta}_0, T_0) = \ddot{\boldsymbol{\xi}}_0$. This acceleration can be obtained by rotating the accelerations measured in the body axes to the NED frame and adding the gravity vector. Furthermore, we assume that the partial derivative of $\boldsymbol{F}$ with respect to $\boldsymbol{v}$ is small compared to the other three partial derivatives. This is commonly referred to as the principle of time scale separation. Combining this with Eq. 2 and 3 we end up with:

$$\ddot{\boldsymbol{\xi}} = \ddot{\boldsymbol{\xi}}_0 + G(\boldsymbol{\eta}_0, T_0/m)(\boldsymbol{u} - \boldsymbol{u}_0) \tag{4}$$

where $\boldsymbol{u} = \begin{bmatrix} \phi & \theta & T/m \end{bmatrix}^T$ and

$$\boldsymbol{G}(\boldsymbol{\eta}, T/m) = \begin{bmatrix} (\mathrm{c}\phi\mathrm{s}\psi - \mathrm{s}\phi\mathrm{c}\psi\mathrm{s}\theta)T/m & (\mathrm{c}\phi\mathrm{c}\psi\mathrm{c}\theta)T/m & \mathrm{s}\phi\mathrm{s}\psi + \mathrm{c}\phi\mathrm{c}\psi\mathrm{s}\theta \\ (-\mathrm{s}\phi\mathrm{s}\psi\mathrm{s}\theta - \mathrm{c}\psi\mathrm{c}\phi)T/m & (\mathrm{c}\phi\mathrm{s}\psi\mathrm{c}\theta)T/m & \mathrm{c}\phi\mathrm{s}\psi\mathrm{s}\theta - \mathrm{c}\psi\mathrm{s}\phi \\ -\mathrm{c}\theta\mathrm{s}\phi T/m & -\mathrm{s}\theta\mathrm{c}\phi T/m & \mathrm{c}\phi\mathrm{c}\theta \end{bmatrix} \tag{5}$$

The measured accelerations, necessary to obtain $\ddot{\boldsymbol{\xi}}_0$, are typically noisy due to vibrations in the airframe introduced by the spinning propellers. Therefore, the accelerations need to be filtered. From the literature, we adopted the use of a second order filter [15], given by:

$$H(s) = \frac{\omega_n^2}{s^2 + 2\zeta\omega_n s + \omega_n^2} \tag{6}$$

This filter also introduces delays in the signal, resulting in delayed acceleration measurements. In previous research [16], we showed that by applying this same filter on the input as well, the input is not incremented further before the result of the previous increment is known. If we denote filtered signals with subscript f and invert Eq. 4, we get the INDI control law for linear accelerations:

$$\boldsymbol{u}_c = \boldsymbol{u}_f + G^{-1}(\boldsymbol{\eta}_0, T_0/m)(\boldsymbol{\nu}_{\ddot{\xi}} - \ddot{\boldsymbol{\xi}}_f) \tag{7}$$

We have replaced $\ddot{\boldsymbol{\xi}}$ with the virtual control $\boldsymbol{\nu}_{\ddot{\xi}}$ to indicate that this is now an input to the equation (the desired acceleration), and we added the subscript c to $\boldsymbol{u}$ to indicate that this is the command that will be sent to the inner loop controller. We also define the *increment* $\widetilde{\boldsymbol{u}} = \boldsymbol{u}_c - \boldsymbol{u}_f$, so clearly Eq. 7 is an *incremental* control law.

III. Implementation

The implementation of the control law given by Eq. 7 is shown in Figure 3. Note how the increment in specific thrust command $\frac{\widetilde{T}}{m}$ is an output of this diagram. This is because the specific thrust is not a control variable in itself, instead the rotors are used to provide a certain thrust. Therefore, the specific thrust will have to go through a second inversion step, to find the rotor angular rate increments that will result in the commanded specific force increment. The rotors are

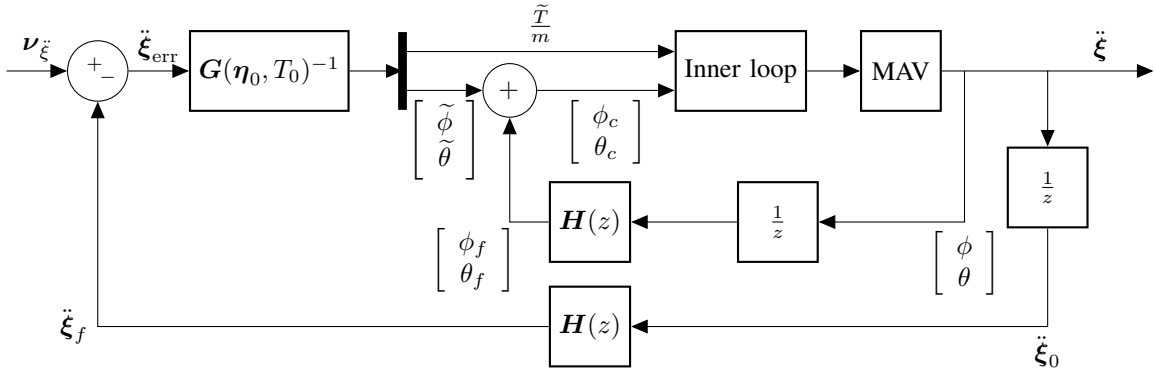

Fig. 3: The outer INDI control structure.

also used by the inner loop INDI controller to control the angular acceleration of the MAV. In order to find rotor increments that satisfy both the increment in angular acceleration as well as the increment in specific thrust, we will expand the inner loop inversion step to include the relation of specific force and rotor angular rates. This way, increments for the angular rates of the rotors can be found that satisfy both the desired increment in angular accelerations as well as the desired increment in specific force.

The inner INDI loop is shown in Figure 4. It was derived in our previous work [16] using similar methods as used in this paper for the outer loop controller. For a complete derivation, including stability analysis, we refer to that paper.

The angular rate of rotor one through four is denoted by the vector $\boldsymbol{\omega}$ and the angular rates of the vehicle by $\boldsymbol{\Omega}$. Note that this diagram contains two different control effectiveness matrices, $\boldsymbol{G}_1$ and $\boldsymbol{G}_2$. $\boldsymbol{G}_1$ is a 4x4 matrix defined as the control effectiveness of the four rotors on the angular acceleration vector and the acceleration in the Z_B axis. $\boldsymbol{G}_2$ is a 4x4 matrix introduced as an extension to $\boldsymbol{G}_1$ to account for changes in the angular momentum of the propellers. Changing the rotational speed of the rotors changes their angular momentum, which produces a torque in the yaw axis. $\boldsymbol{G}_2$ therefore has one row of nonzero values, corresponding to yaw axis.

A. Estimation of the Specific Thrust

Throughout the derivation of the outer loop INDI controller, we made use of the specific thrust $\frac{T}{m}$, for instance in the matrix $G(\boldsymbol{\eta}, T/m)$. In this paper, we assumed that the aerodynamic forces in the z_B direction are small compared to the thrust. Then the specific thrust can be approximated by the specific force measured by the onboard accelerometer in the z_B direction. This assumption only holds around hover. A better way to obtain the specific thrust would be to model the thrust/rotational rate curve of the propellers and measure the mass of the drone. This will be done in future work.

Furthermore, since the propellers have a quadratic thrust curve, their control effectiveness changes depending on their current rotational rate. In this paper, we assume that the control effectiveness of the rotors with respect to the specific force can be approximated by a static one. In future research, we will investigate the benefits of using the thrust/rotational rate curve of the propellers in the controller.

B. Position Control

The acceleration of the vehicle is accurately controlled by the system shown in Figure 3. To control the position of the MAV, an acceleration reference needs to be passed to the outer INDI controller that will steer the drone towards its target position. This can be done by a Proportional Derivative (PD) controller of the form:

$$\boldsymbol{\nu}_{\ddot{\xi}} = D(P\boldsymbol{\xi}_{\text{err}} - \dot{\boldsymbol{\xi}}) \tag{8}$$

The gains of this PD controller were manually tuned. They depend mainly on two things: the update rate of the position estimate and the speed of the inner loop controller, which is only dependent on the actuator dynamics. This is the case because all other components are inverted in the inversion step of the inner and outer loop.

C. Filtering

The measured accelerations are filtered to remove noise. This filtering also introduces a delay. To make sure we only increment the control signal when we are able to measure the result of the previous increment, the control signal and the measurement need to be synchronized by applying the same filter, and hence the same delay. For the roll and pitch controls this is straightforward, as is shown in Figure 3. The specific thrust increment is added to the rotor angular rates after a second inversion step in Figure 4. Therefore, the rotor angular rates should also be filtered with the same filter.

However, the angular rates of the rotors are also used to control the angular acceleration of the vehicle. This is done with the inner INDI control loop shown in Figure 4. Here the increment of the rotor angular rates is calculated from the measured angular acceleration, which is obtained from the gyroscopes. This measurement is also noisy, and needs to be filtered. Because of this, the angular rates of the rotors should be filtered with the same filter.

Since both the inner and the outer loop make use of the same actuators, the rotational rate of the rotors, their filters need to be the same. For the experiment, we chose a filter with a $\omega_n = 50$ rad/s and $\zeta = 0.55$. Choosing a lower

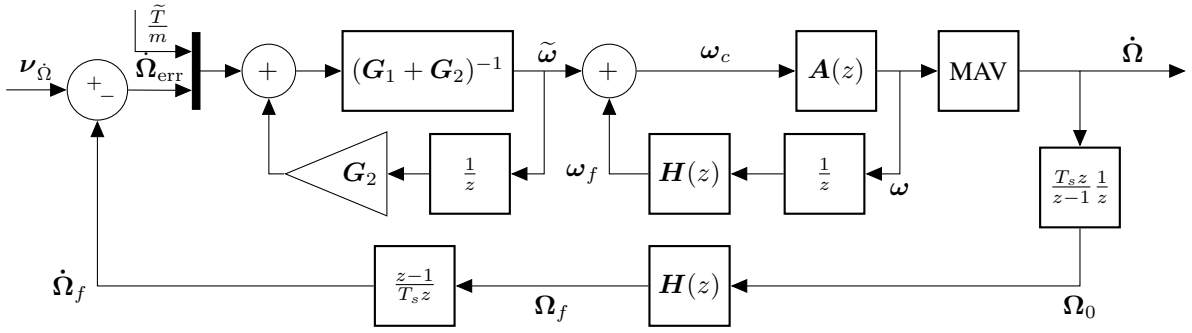

Fig. 4: The inner INDI control structure.

cutoff frequency will result in less noise, but more delay. This means that it will take longer for disturbances to be measured and counteracted. Choosing a higher cutoff frequency will have the reverse effect, more noise will end up in the control signals but disturbances are counteracted faster.

D. Linearization

The control of the acceleration is nonlinear in terms of the inputs, especially roll and pitch, as can be seen from Equation 2. In Equation 5 it can even be seen that some of the control derivatives can change sign, for instance $\frac{\partial \ddot{z}}{\partial \phi}$ for different values of ϕ.

What this means in practice is that if the increments in the input are large, because suddenly a large lateral acceleration is required, they will result in a different acceleration than intended. A solution may be to implement a nonlinear method of finding increments in the input that give the desired increment in the acceleration. In this paper, we solved this issue by bounding the acceleration increment such that the resulting change in inputs can still be approximated linearly.

IV. Experimental Setup

The goal of the experiment is to test how well the controller can handle gust disturbances. The experiment will be performed indoors, such that there is a controlled environment in which repeatable experiments can be performed. The drone will be commanded to fly back and forth between two waypoints at the same altitude, which are about one meter apart in the east direction. The source of the disturbance is a Master DF30P 465 W fan placed in front of one of the waypoints, blowing towards north. The fan produces a non-uniform wind with airspeeds ranging from 1.3 m/s in the center to 4.0 m/s towards the edge of the fan, which was measured 1 m downstream. When the drone reaches the waypoint with the fan, it will suddenly experience the wind. When the drone leaves the waypoint, it will fly out of the wind again. The drone will spend eight seconds at each waypoint and repeat this three times.

The performance of the INDI controller will be compared to a PID controller which is manually tuned to give the fastest response possible. This PID controller also makes use of the inner loop INDI controller for attitude control, but it does not use the outer loop INDI controller. The P, I and D gains work directly on the position and velocity to produce a reference roll, pitch and thrust. For the PID controller, there is a trade-off to be made. By increasing the integral gain, faster offset compensation can be obtained. This way the quadrotor can adjust to the disturbance of the fan faster. However, by increasing the integral gain, the quadrotor will have more overshoot in reference tracking tasks such as sudden position changes. This trade-off is non-existent for the INDI controller.

The MAV used for the experiments is the Bebop quadrotor from Parrot. Instead of the stock firmware, it is running the Paparazzi open source autopilot system. The control algorithm, as well as the onboard accelerometer and gyroscope, were running at 512 Hz. An infrared motion tracking system called 'Optitrack' was used to obtain position information. This system can measure the drone's position with millimeter accuracy at a frequency up to 120 Hz. But because we want the experiment to be realistic for outside scenarios and since most Global Positioning System (GPS) modules can only provide position updates at four Hz, the data was only sent to the drone at a frequency of four Hz.

The Optitrack system can deliver better accuracy than a GPS module, so it might seem that the experiment is still not realistic, regardless of the low update rate. However, if the GPS position estimate is not accurate, the drone will fly to an erroneous position, where the estimated position equals the reference position. At this position, disturbances will still be counteracted the same way, as this is done using the accelerometer measurement, independent of the position. The more accurate the GPS module is, the more accurate the (real world) position tracking will be, but the disturbance rejection properties will be the same. Outdoor experiments are considered future work, but preliminary tests showed promising results.

The source code can be found online on GitHub[1], so the experiment is easy to reproduce.

V. Results

For the outer loop INDI experiment, Figure 5 shows the acceleration of the MAV in the North and East directions respectively. The acceleration signal shown is filtered on the

[1]https://github.com/EwoudSmeur/paparazzi/tree/IROS2016_experiment

drone with the second order filter given by Eq. 6 with $\zeta = 0.55$ and $\omega_n = 50$ rad/s. The East axis shows the acceleration in the direction orthogonal to the disturbance. Here we see accurate tracking of the acceleration reference. In the North axis, we can see the effect of the wind on the acceleration at 35 s and 43 s when the MAV enters and leaves the wake of the fan.

Figure 5 also shows the position of the quadrotor during the experiment for the outer loop INDI controller. It can be seen that the INDI controller is able to track step responses with minimal overshoot. From the top figure it can be observed that entering and leaving the fan's wake, for instance at 35 s and 45 s, typically results in a position change of about five cm. This error is rejected in two seconds after its occurrence.

Note the offset that can be observed in Figure 5 for the North position of the drone with INDI controller. In our previous work on the inner loop attitude control we did not see such offsets in the attitude angles. The reason for this is that the angular acceleration measurement was bias-free, as it was derived from the angular rate measurement. For the linear acceleration, we rely on a direct measurement. Sensor drift or an error in the attitude estimation can lead to errors in the estimate of the acceleration. In the complete interval of [30,80] s in the x axis, the average measured acceleration was -0.08 m/s^2. However, because of estimation errors there is no real acceleration and a bias in the position is the result. This problem can be solved by estimating the accelerometer bias through the derivative of the speed estimate, which will be considered in future work.

Compare this with the position of the quadrotor during the experiment for the PID controller in Figure 5. In the East axis it can be seen that the relatively large integral gain resulted in some overshoot of the step reference, which did not happen without the integral gain. However, in the North axis it can be observed that even with this large integral gain, the quadrotor is blown away more than half a meter and it takes about five seconds for it to get back to the reference. The moment it flies back to the first waypoint it overshoots in the other direction, because now it suddenly flies out of the fan's wake.

Because the fan was blowing toward the North, the average position error in the North direction is a measure of the performance. From Figure 5, the average error in x is 6.4 cm for the INDI controller and 19.3 cm for the PID controller. As was mentioned before, the position error for the INDI controller is mostly due to the acceleration bias. Estimation of this bias can result in even better performance.

Finally a top view of the experiment is depicted in Figure 6. It shows the track of the quadrotor for the experiments with the INDI and PID controller for the interval of [30,50] s and [20,40] s respectively. The figure shows how well the INDI controller can reject the disturbance of the fan compared to a traditional PID controller.

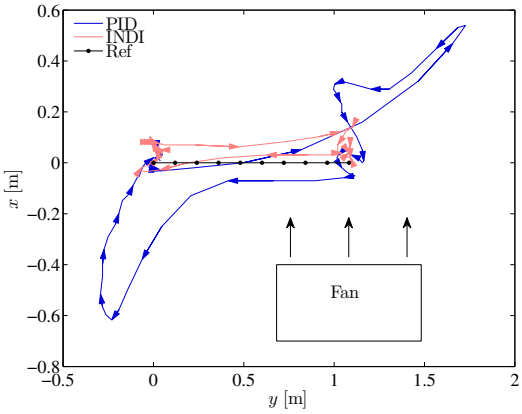

Fig. 6: Top view of the trajectories of the INDI and PID controller (best viewed in color).

VI. Conclusions

We have generalized Incremental Nonlinear Dynamic Inversion (INDI) for the control of linear accelerations of a quadrotor subject to disturbances. The experiments show that the performance of the INDI controller is three times better than that of a traditional Proportional Integral Derivative (PID) controller in terms of average position error. In the experiments, the quadrotor received four Hz position updates, which means that the technique can readily be applied outdoors with standard GPS modules. This outer loop INDI controller enables Micro Aerial Vehicles to perform tasks that require accurate position control under gusty conditions, such as flying near obstacles and entering a building through a window.

References

[1] A. Ryan and J. Hedrick, "A mode-switching path planner for UAV-assisted search and rescue," in *44th IEEE Conference on Decision and Control*, 2005, p. pp. 14711476.

[2] J. Kim and S. Sukkarieh, "Airborne simultaneous localisation and map building," in *IEEE International Conference on Robotics and Automation*, 2003.

[3] D. Mellinger, N. Michael, and V. Kumar, "Trajectory generation and control for precise aggressive maneuvers with quadrotors," *The International Journal of Robotics Research*, vol. 31, no. 5, pp. 664–674, 2012.

[4] K. Alexis, G. Nikolakopoulos, and A. Tzes, "Constrained-Control of a Quadrotor Helicopter for Trajectory Tracking under Wind-Gust Disturbances," in *IEEE Mediterranean Electrotechnical Conference*, 2010.

[5] S. Shen, N. Michael, and V. Kumar, "Autonomous Multi-Floor Indoor Navigation with a Computationally Constrained MAV," in *International Conference on Robotics and Automation*, May 2011.

[6] N. Sydney, B. Smyth, and D. A. Paley, "Dynamic control of autonomous quadrotor flight in an estimated wind field," in *IEEE Conference on Decision and Control (CDC)*, December 2013.

[7] S. L. Waslander and C. Wang, "Wind Disturbance Estimation and Rejection for Quadrotor Position Control," in *AIAA Infotech@Aerospace Conference and AIAA Unmanned...Unlimited Conference*, April 2009.

[8] F. Schiano, J. Alonso-Mora, K. Rudin, P. Beardsley, R. Siegwart, and B. Siciliano, "Towards Estimation and Correction of Wind Effects on a Quadrotor UAV," in *International Micro Air Vehicle Conference and Competition (IMAV)*, August 2014.

[9] R. C. Gardner and J. S. Humbert, "Comparative Framework for Maneuverability and Gust Tolerance of Microhelicopters," *Journal of Aircraft*, vol. 51, no. 5, pp. 1546–1553, 2014.

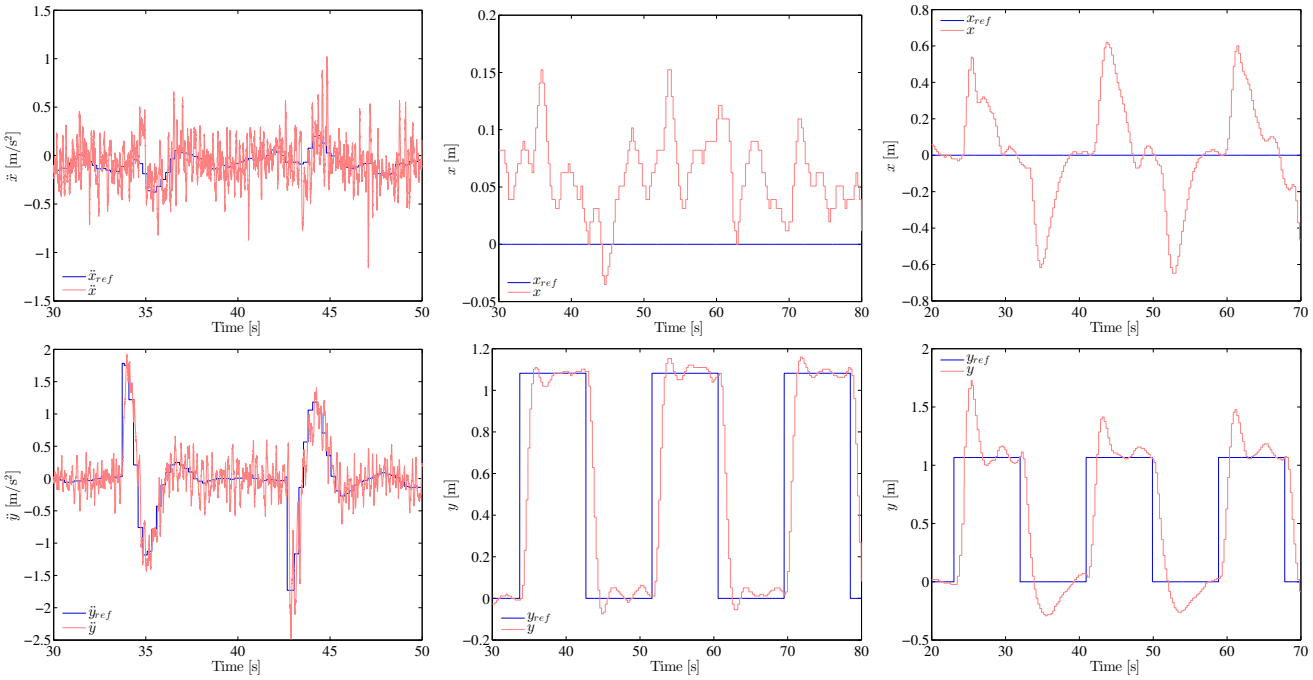

Fig. 5: The top row shows the results in the North axis and the bottom row in the East axis. The left figures are the acceleration for the INDI controller. In the middle the corresponding position is shown. The right figures show the position for the PID controller.

[10] G. M. Hoffmann, H. Huang, S. L. Waslander, and C. J. T. c, "Precision flight control for a multi-vehicle quadrotor helicopter testbed," *Control Engineering Practice*, vol. 19, no. 9, pp. 1023–1036, 2011.

[11] P. Simplicio, M. Pavel, E. van Kampen, and Q. Chu, "An acceleration measurements-based approach for helicopter nonlinear flight control using Incremental Nonlinear Dynamic Inversion," *Control Engineering Practice*, vol. 21, no. 8, pp. 1065–1077, aug 2013.

[12] S. Sieberling, Q. P. Chu, and J. A. Mulder, "Robust Flight Control Using Incremental Nonlinear Dynamic Inversion and Angular Acceleration Prediction," *Journal of Guidance Control and Dynamics*, vol. 33, no. 6, pp. 1732–1742, 2010.

[13] J. Wang, T. Raffler, and F. Holzapfel, "Nonlinear Position Control Approaches for Quadcopters Using a Novel State Representation," in *Guidance, Navigation and Control Conference*. AIAA Paper 2012-4913, 2012.

[14] G. Hattenberger, M. Bronz, and M. Gorraz, "Using the Paparazzi UAV System for Scientific Research," in *International Micro Air Vehicle Conference and Competition (IMAV)*, 2014.

[15] B. J. Bacon, A. J. Ostroff, and S. M. Joshi, "Reconfigurable NDI Controller Using Inertial Sensor Failure Detection & Isolation," *IEEE Transactions On Aerospace And Electronic Systems*, vol. 37, no. 4, pp. 1373–1383, Oct 2001.

[16] E. J. J. Smeur, Q. P. Chu, and G. C. H. E. de Croon, "Adaptive Incremental Nonlinear Dynamic Inversion for Attitude Control of Micro Aerial Vehicles," *Journal of Guidance, Control, and Dynamics*, vol. 39, no. 3, pp. 450–461, March 2016.